

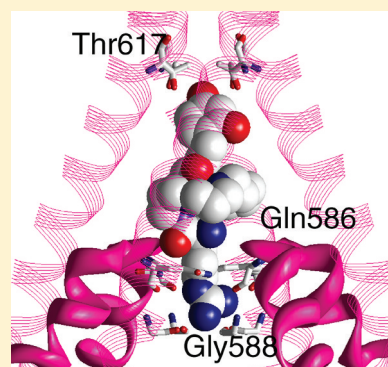
# Argiotoxin in the Closed AMPA Receptor Channel: Experimental and Modeling Study

Oleg I. Barygin,<sup>†</sup> Eugene V. Grishin,<sup>‡</sup> and Denis B. Tikhonov<sup>\*,†</sup>

<sup>†</sup>I.M. Sechenov Institute of Evolutionary Physiology and Biochemistry, Russian Academy of Sciences, St. Petersburg, Russia

<sup>‡</sup>M.M. Shemyakin and Yu.A. Ovchinnikov Institute of Bioorganic Chemistry, Russian Academy of Sciences, Moscow, Russia

**ABSTRACT:** Binding of argiotoxin in the closed state of Ca<sup>2+</sup>-permeable AMPA receptor channels was studied using electrophysiological and molecular modeling approaches. Experimental study unambiguously revealed that argiotoxin is trapped in the closed AMPA receptor channels after agonist dissociation. Docking of the argiotoxin to the channel model based on recently published X-ray structure demonstrated that the drug can be effectively accommodated in the cavity of the closed channel only if the terminal moiety of the molecule penetrates in the narrow portion of the pore below the selectivity filter. Combining these results, we conclude that the selectivity filter of the AMPA receptor channels is not sterically occluded in the closed state.



Ionotropic glutamate receptors are ligand-gated ion channels that mediate the postsynaptic current in response to a neurotransmitter binding. However, it was shown that the glutamate-gated ion channels differ markedly from nicotinic acetylcholine receptors and GABA<sub>A</sub> receptors. It was also demonstrated that glutamate-gated channels are homologous to the family of P-loop channels, which includes potassium, sodium, and calcium channels.<sup>1</sup> While the general similarity between glutamate-gated channels and other members of the superfamily is commonly accepted, the degree of resemblance among the channels is still being discussed; in particular, under question is how similar the mechanisms of gating are. Some studies have provided evidence in favor of a rather close resemblance,<sup>2</sup> whereas other investigations have revealed obvious differences.<sup>3,4</sup> Recent crystallization of the AMPAR channel clearly demonstrated a remarkable similarity between the closed states of the K<sup>+</sup> KcsA channel and the AMPAR channel.<sup>5</sup>

However, the structure of an open AMPAR channel is still unknown, and it remains impossible to draw any conclusions on the similarity between the open states. In such circumstances, the exact mechanisms of AMPAR channel gating remain unclear. Because a tight bundle of the C-halves of the M3 segments unambiguously corresponds to a closed gate, the diverging of these segments during gating seems clear. This gating mechanism agrees with numerous mutational studies and with the data on use-dependent drug binding.<sup>6–9</sup> However, it should be noted that K<sup>+</sup> channels are also gated at the level of the selectivity filter.<sup>10,11</sup> Most likely, gating at the selectivity filter corresponds to the C-type inactivation of the K<sup>+</sup> channels.<sup>12</sup> Recently, a coupling between the gates at the S6 segments' level and at the level of the selectivity filter has been

revealed.<sup>13</sup> Some studies have also suggested gating of ionotropic glutamate receptors at the level of the selectivity filter.<sup>14,15</sup> Unfortunately, the selectivity filter region is not resolved in the available X-ray structure of the AMPAR channel, and we cannot judge if it is in a conducting or nonconducting state while the channel is closed. In the absence of X-ray data on the conformation of the selectivity filter, indirect approaches can be used. Herein, we report the results of molecular modeling of argiotoxin binding to the AMPAR channel in combination with electrophysiological analysis of the mechanism of argiotoxin action. The toxin was initially isolated from the venom of *Argiope lobata* spider, and it was found that argiotoxin blocks the ion channels of postsynaptic glutamate receptors in insect neuromuscular junction and also blocks mammalian ionotropic glutamate receptors.<sup>16,17</sup> This polyamine-containing toxin was used as a pharmacological tool in several studies, and many synthetic derivatives were synthesized and tested in order to analyze their structure–activity relationships and to reveal topography of the binding sites in the NMDAR and AMPAR channels.<sup>18–26</sup> Being a large-size molecule, the argiotoxin is suitable for the present study of the closed AMPAR channel because it allows us to reveal the steric limitations of binding in the channel cavity.

## MATERIALS AND METHODS

Wistar rats (12–17 days old) were anesthetized with urethane and then decapitated. Maximum efforts were made to minimize

**Received:** April 22, 2011

**Revised:** July 10, 2011

**Published:** August 15, 2011



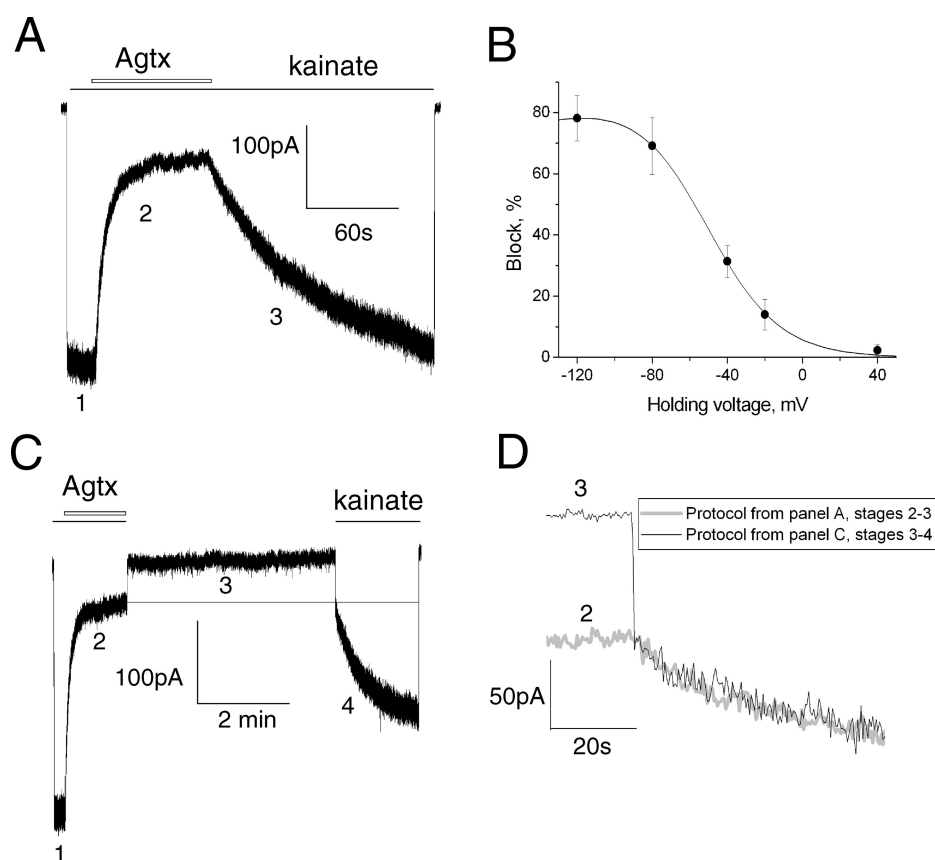


**Figure 1.** Action of argiotoxin on the  $\text{Ca}^{2+}$ -permeable AMPA receptor channels in giant striatal interneurons. (A) At  $-80$  mV holding voltage the kainate-evoked current (1) is blocked by  $0.5 \mu\text{M}$  argiotoxin (2). The inhibition is reversible (3). (B) Voltage dependence of the AMPAR inhibition by  $0.5 \mu\text{M}$  argiotoxin. A negligible block at positive voltages suggests the lack of a voltage-independent action. (C) Trapping of argiotoxin in a closed AMPAR channel. The initial response to kainate (1) is 75% blocked by  $0.5 \mu\text{M}$  of argiotoxin (2). Next, both kainate and the toxin are removed (3). The testing response to kainate (4) after 5 min has a fast onset to a level almost equal to the equilibrium response at the end of stage 2. The development of a further response has slow kinetics, which reflects the argiotoxin unbinding after channel opening. The fact that no recovery from the block was observed during 5 min in the absence of kainate strongly suggests the trapping of argiotoxin in the closed AMPAR channels. (D) Superimposition of the made from the same cell recordings of the trapping protocol (panel C, stages 3 and 4) and of the recovery from argiotoxin-induced block in the presence of kainate (panel A, stages 2 and 3). The kinetics of recovery in these experiments coincides.

the number and sufferings of animals used. The rats' brains were removed quickly and cooled to  $2-4^\circ\text{C}$  in an ice bath. Transverse striatal slices ( $250 \mu\text{m}$  thick) were prepared using a vibratome (Campden Instruments Ltd., Loughborough, UK) and stored in a solution containing (in mM): NaCl 124, KCl 5,  $\text{CaCl}_2$  1.3,  $\text{MgCl}_2$  2.0,  $\text{NaHCO}_3$  26,  $\text{NaH}_2\text{PO}_4$  1.24, D-glucose 10, aerated with carbogen (95%  $\text{O}_2$ , 5%  $\text{CO}_2$ ). Single neurons were freed from slices by vibrodissociation. Antagonism of  $\text{Ca}^{2+}$ -permeable AMPAR was studied on striatal giant interneurons, which were identified by their shape and size. They have a large ( $>25 \mu\text{m}$ ) soma of polygonal shape, whereas principal cells are significantly smaller and almost spherical. All experiments were performed at room temperature ( $22-24^\circ\text{C}$ ). The whole-cell patch clamp technique was used for recording membrane currents generated in response to applications of  $100 \mu\text{M}$  kainate. Currents were recorded using an EPC-8 amplifier (HEKA Electronics, Lambrecht, Germany), filtered at 5 kHz, sampled, and stored on a personal computer. Drugs were applied using the RSC-200 perfusion system (BioLogic Science Instruments, Claix, France) under computer control. The extracellular solution contained (in mM): NaCl 143, KCl 5,  $\text{MgCl}_2$  2.0,  $\text{CaCl}_2$  2.5, D-glucose 18, HEPES 10 (pH was adjusted to 7.3 with HCl). The pipet solution contained (in mM): CsF 100, CsCl 40, NaCl 5,  $\text{CaCl}_2$  0.5, EGTA 5, HEPES

10 (pH was adjusted to 7.2 with CsOH). Drugs were purchased from Sigma. All experimental data are presented as means  $\pm$  SD estimated from at least four experiments.

All calculations were performed using the ZMM program. The nonbonded energy was calculated using the AMBER force field<sup>27</sup> with a cutoff distance of  $8 \text{ \AA}$ , and the hydration energy was calculated using the implicit solvent method.<sup>28</sup> Electrostatic interactions were calculated using the distance-dependent dielectric function, and the atomic charges of argiotoxin were calculated by the semiempirical method AM1<sup>29</sup> using MOPAC. The MCM method<sup>30</sup> was used to optimize the model. During energy minimizations, alpha carbons of the P-helices were constrained to corresponding positions of the template using pins. A pin is a flat-bottom energy function, which allows an atom to deviate penalty-free up to  $1 \text{ \AA}$  from the template and imposes a penalty of  $10 \text{ kcal mol}^{-1} \text{ \AA}^{-2}$  for deviations  $>1 \text{ \AA}$ . The model was MC-minimized until 2000 consecutive minimizations did not decrease the energy of the apparent global minimum.

## RESULTS

**Experimental Analysis.** The action of the argiotoxin on the AMPAR channel has been the subject of many studies,<sup>31</sup> and it was demonstrated that argiotoxin selectively blocks  $\text{Ca}^{2+}$ -

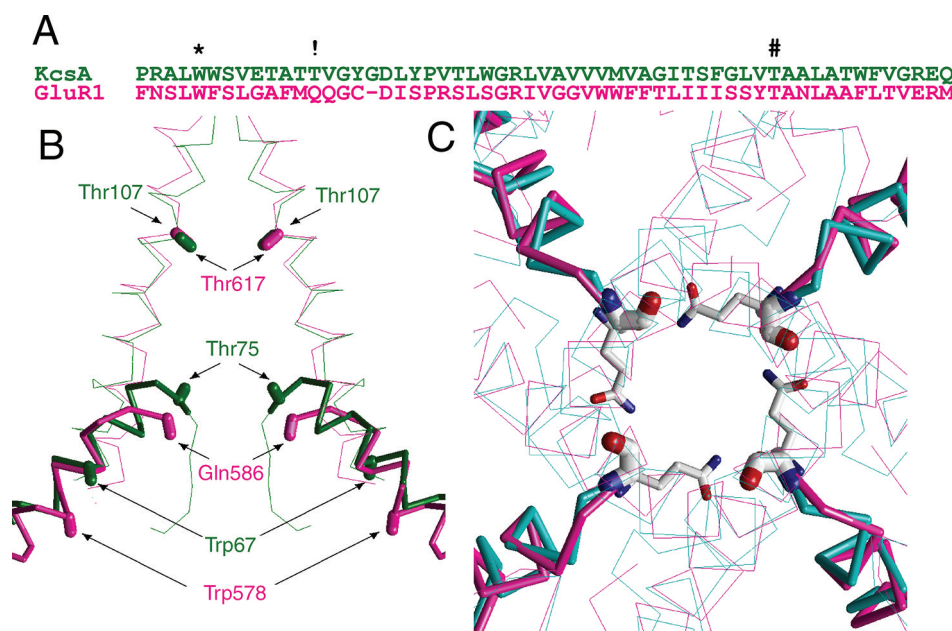


**Figure 2.** Modeling of the AMPAR channel. (A) Aligned sequences of KcsA K<sup>+</sup> and AMPAR channels. Position of the selectivity filter residues (Q/R site) is marked by “!”. Position of homologous Trp67 in KcsA and Trp587 in AMPAR is marked by “\*”. Position of the closed gate (Thr617 and Thr107) is marked by “#”. (B) Superimposition of the KcsA (PDB code 1BL8) and GluRB (PDB code 3KG2) structures. Structural alignment was performed by minimizing rmsd of the inner helix alpha carbons. With this alignment, the pore helix of GluRB appears to be shifted by one turn relative to the position in KcsA and other potassium channels. This is reflected in the location of Trp578 relative to the homologous Trp67 in KcsA. (C) Superimposition of the X-ray structure of GluRB and its model. The selectivity filter (Gln586) in the X-ray is shown by thin sticks. In the model, the side chains (thick sticks) were assumed to form the cyclic motif due to the intersubunit H-bonds.

permeable GluA2-lacking AMPAR channels. The action was found to be voltage- and use-dependent, suggesting open channel block as the primary mechanism of action. The fact that mutations at the Q/R site control the argitoxin sensitivity confirmed this view. For many AMPAR channel blockers, the trapping mechanism was proven.<sup>32,33</sup> These compounds can enter the AMPAR channel only when it is in an open state. However, after the channel has closed, the blocking molecules remain trapped in the closed channel and cannot leave until it opens again.

Initially, we analyzed the argitoxin action on steady-state currents evoked by an application of 100  $\mu$ M weakly desensitizing AMPAR agonist kainate (Figure 1A). The IC<sub>50</sub> value at -80 mV was estimated as 0.19  $\mu$ M from the concentration dependence of the block. In our experiments argitoxin blocked the AMPAR channel in a voltage-dependent manner. The electrical depth of the binding site was estimated from analysis of the action of 0.5  $\mu$ M argitoxin at different holding voltages using the Woodhull model. Fitting the voltage dependence data suggested a  $z\delta$  value of 0.93 (Figure 1B). These data are in agreement with previous studies.

Despite previous studies concerning the action of argitoxin on AMPAR channels, there is no unambiguous evidence of its trapping in the closed channels. Therefore, we performed experiments to address this point. Figure 1C shows the experiment that revealed the trapping mechanism of the block. After the recording of the control response to 100  $\mu$ M kainate, 0.5  $\mu$ M argitoxin was applied for 90 s and produced a  $71 \pm 7\%$  block. Next, both kainate and argitoxin were simultaneously removed from the solution. A testing kainate application was performed after 5 min, and it was clearly seen that the recovery from block during the interval between the removal of the toxin and the kainate and the testing kainate application did not

exceed 5%. The recovery from block developed during the kainate testing application. A  $64 \pm 9\%$  recovery was reached during 2 min of the kainate application. The data indicate that recovery from argitoxin block takes place only in the presence of kainate, i.e., that the toxin molecule is trapped in the closed AMPAR channel when kainate is removed.

It is possible that the binding mode of the toxin in a closed channel differs from that in an open channel. In this case the stability of the drug-channel complex should also depend on the channel state. If it were so, the kinetics of recovery from block would be different in the protocols shown in the Figure 1A,C. In the continuous presence of an agonist the toxin is bound predominantly to the open channels. In the trapping protocol the toxin is bound to the closed channels. However, the kinetics of recovery was found to be the same in both cases (see Figure 1D). The time constant was  $46 \pm 9$  s in the continuous presence of an agonist and  $42 \pm 8$  s in the trapping protocol. Thus, our experiments do not support the idea of significantly differing binding modes of argitoxin in the open and the closed states of the AMPAR channel.

**Molecular Modeling.** The AMPAR channel structure was modeled according to the recent X-ray data.<sup>5</sup> The unresolved selectivity filter residues were modeled according to our previous studies,<sup>2</sup> which suggested a cyclic motif of the Q/R site stabilized by the side chain to backbone intersubunit H-bonds. The position of the Q/R site residues (Gln586) in the X-ray structure<sup>5</sup> generally agrees with our prediction. Thus, alpha carbons deviate from the prediction<sup>2</sup> by 2.1 Å only. The backbone carbonyl oxygen and side chains in the X-ray structure are directed toward neighboring subunits, allowing closure of the proposed<sup>2</sup> intersubunit H-bonds (Figure 2C). In our model,<sup>2</sup> the backbone oxygen of Gly588 faces the pore and Asp590 forms the intrasubunit bond with Trp578. It should be

**Table 1. Energetics of Different Binding Modes of Argiotoxin<sup>a</sup>**

argiotoxin binding model	energy (kcal/mol)			
	total	intraligand	intrareceptor	ligand–receptor
channel model with wide selectivity filter				
free docking (94)	−2442 ± 3	−7 ± 1	−2393 ± 5	−45 ± 4
constrained docking (87)	−2398 ± 4	−5 ± 2	−2360 ± 4	−37 ± 5
remote drug (66)	−2426 ± 3	−19 ± 2	−2405 ± 2	0
channel model with occluded selectivity filter				
free docking (97)	−2220 ± 3	−9 ± 2	−2174 ± 4	−41 ± 4
remote drug (84)	−2217 ± 4	−19 ± 2	−2198 ± 3	0

<sup>a</sup>The data are presented as mean ± SD in the ensemble of low-energy structure obtained by the two-step optimization. The total numbers of structures in the ensembles are shown in parentheses.

noted that in the AMPAR channel the X-ray position of Trp578 significantly differs from the position of the homologous Trp67 residue in the KcsA K<sup>+</sup> channel<sup>34</sup> (Figure 2A,B). This obvious difference does not agree with the strong similarity between AMPAR and K<sup>+</sup> channels claimed by Sobolevsky and colleagues.<sup>5</sup> From the comparison of the X-ray structures, it seems that the entire pore helix (helical part of M2) is shifted about 1 helix turn from the position seen in the K<sup>+</sup> channels. As noted by the authors,<sup>5</sup> “Within the pore lays the M2 helix, positioned largely on the basis of tube-shaped electron density and the anomalous difference density peak from the SeMet-labeled Gln 586 to Met (Q/R site) mutant.” Because of the shift, the cavity in the AMPAR X-ray structure is larger than in K<sup>+</sup> channel structure (Figure 2B). Since one of the goals of our modeling was to estimate the steric limitations of drug binding in the cavity of a closed AMPAR channel, we used the same pore helix geometry as in the original AMPAR X-ray structure.<sup>5</sup>

The amino acid sequences of AMPAR channels are highly conservative within the pore region. The key difference determining pharmacological sensitivity and permeability is Gln to Arg substitution in the selectivity filter (Q/R) site. Gln residue provides Ca<sup>2+</sup> permeability as well as sensitivity to cationic blockers including the argiotoxin.<sup>1</sup> The positively charged Arg residue in GluA2 subunit is responsible for low channel conductance and Ca<sup>2+</sup> permeability and for low sensitivity to argiotoxin of the GluA2-containing AMPAR channels. This validates the use of the AMPAR X-ray structure<sup>5</sup> with the Gln586 residue for modeling of argiotoxin action on the Ca<sup>2+</sup>-permeable AMPARs.

The model was optimized using the MCM protocol to find unresolved side-chain conformations. The energetics of the model with a remote argiotoxin molecule is shown in the Table 1. In these calculations the drug molecule was placed 50 Å from the channel to exclude the channel–drug interactions and to find intrinsic energetically optimal conformations of both the channel model and the drug. Next, the argiotoxin molecule (Figure 3A) was placed in the central cavity. A total of 10 000 orientations of the toxin were randomly generated, and each structure was optimized using the MCM protocol. During this step, the backbone of the channel model was kept rigid to prevent model disordering by high-energy contacts in the randomly generated starting point. In the next step, the 100 lowest energy complexes found were further optimized with variable backbone torsions of the model and bond angles of the toxin. The low-energy structures found at the second stage of optimization (all structures possessing energy within 10 kcal/mol from the global energy minimum) were considered as possible complex conformations. This two-stage MCM docking

protocol provides effective exploration of the binding site and allows finding the lowest energy binding modes of a drug.<sup>35</sup>

Table 1 demonstrates that the intraligand and intrareceptor energies in a complex are higher than in the situation with a remote argiotoxin molecule. This is obvious because the drug–channel interactions result in some deviations of the toxin molecule and the channel from their optimal conformations. However, the interaction energy compensates this increase of internal energies. The total complex energy was found 17 kcal/mol better than the energy of a system with a remote drug molecule (Table 1). The list of residues significantly contributing to the binding energy is shown in Figure 4A. These residues form the internal shell of the channel cavity (Figure 4B). The pattern of argiotoxin-sensing residues revealed by the modeling agrees well with the results of the SCAM<sup>3,36</sup> and mutational experiments with glutamate receptor channel blockers.<sup>37,38</sup> In particular, one of the most contributing residues is the Gln586 (Q/R site). In the GluA2 subunit, this position is occupied by Arg residue. The electrostatic repulsion between the positively charged Arg side chain, and the cationic toxin clearly explains the low sensitivity of the GluA2-containing AMPAR to argiotoxin. The residues L610, I613, and T617 face the channel cavity in the X-ray structure and significantly interact with the drug in our argiotoxin binding model. Cys mutants in these positions are labeled by MTS reagents in the absence of glutamate. More surprising is high contribution of the W610, which face the pore near the bottom of the cavity. This position is not labeled in SCAM,<sup>3</sup> and it is not pore facing with the KcsA-like positions of the P-loops.

In all low-energy structures obtained, the toxin adopts a semifolded conformation (Figure 3B). Carbonyl oxygens of the toxin molecule form intramolecular H-bonds with one or two amino groups. As a result of this H-bonding, the folded part of the toxin molecule forms a “head” with polar groups buried and the hydrophobic surface exposed. The head fills the channel cavity and interacts with the hydrophobic pore-exposed side chains. In all structures, the terminal guanidinium group was not involved in the pattern of intramolecular H-bonds but formed an extended “tail”. The tail permeated through the Q/R site and reached the ring of the pore-exposed oxygens belonging to the Gly588 residues (Figure 3B). This binding mode is in agreement with our earlier proposals.<sup>21,22,39</sup> For our study, it was important that a significant part of the argiotoxin molecule bound in the closed channel was inside the narrow channel part below the selectivity filter. In other words, for this type of binding in a closed channel, it is necessary that the selectivity filter must not be collapsed. Furthermore, the



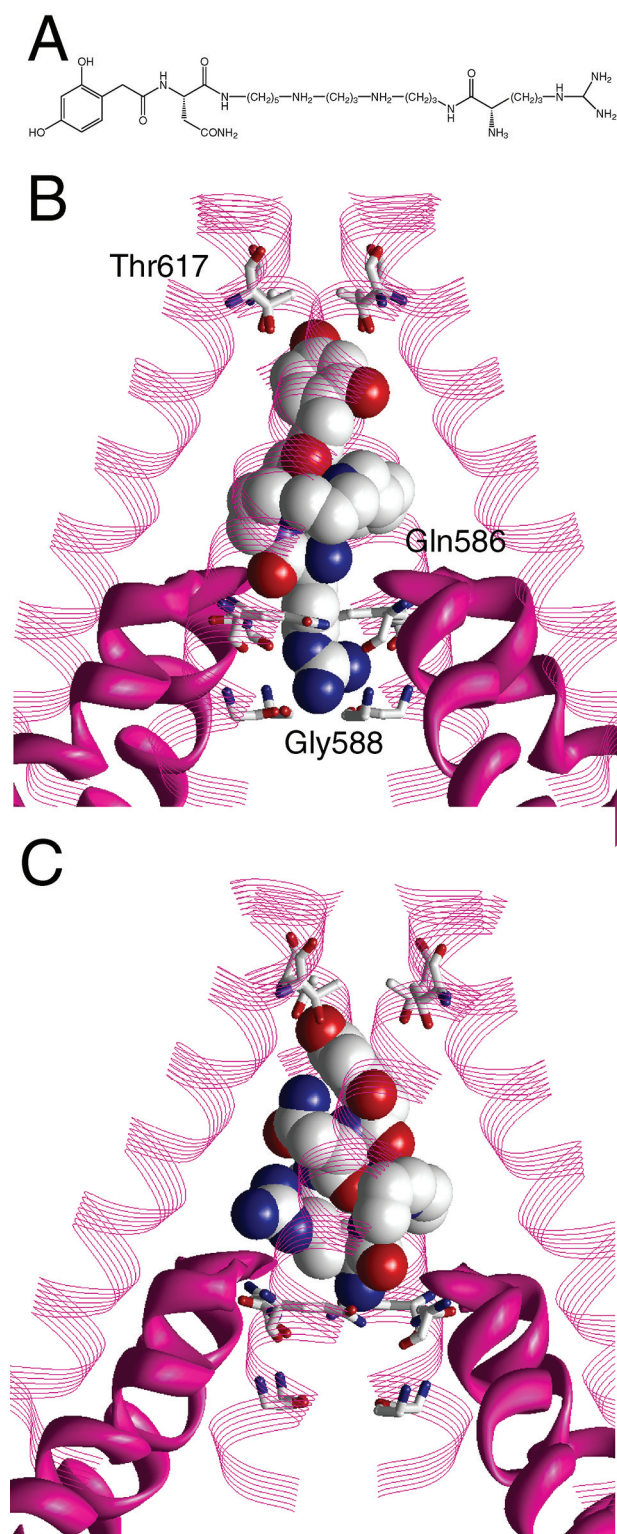


**Figure 3.** Docking of argitoxin to the AMPAR channel model. (A) Chemical structure of the argitoxin. (B) Result of the unconstrained docking (the lowest energy structure is shown). The folded headgroup is accommodated in the cavity between the closed gate (Thr617) and the selectivity filter (Gln586). The terminal charged group penetrates deeper into the narrow channel portion and reaches the Gly588. (C) Result of constrained docking (the lowest-energy structure is shown). The entire molecule was forced to remain between Thr617 and Gln586 by a constraint.

channel must be wide enough to accommodate the tail of the toxin.

While the accommodation of the tail in the narrow channel part was necessary for the energetically optimal binding mode of argitoxin found in our calculations, this could be an artificial result because the conformation of the narrow part was modeled without a precise X-ray template structure. To check the possibility that argitoxin could be accommodated in a closed AMPAR channel without placing its tail in the narrow part, we performed additional calculations.

To prevent the permeation of the terminal part of argitoxin molecule below the selectivity filter, we imposed an additional constraint, which stopped the argitoxin molecule from crossing the plane of alpha carbons of Gln586. In the structure obtained through the docking procedure, the drug molecule was found completely folded (Figure 3C). In this binding mode, the energy of the ligand–channel interaction was slightly increased but remained negative (see Table 1). However, the intrareceptor interactions became 47 kcal/mol higher. The partitioning of the channel energy increase (Figure 4C,D) shows that most of the changes occur for the residues that surround the cavity and at the region of the gate (the C-part of M3 segments). This is due to the steric limitations of the channel cavity. To accommodate the entire argitoxin molecule in the cavity between the closed gate and the selectivity filter, the channel must adopt an unfavorable conformation. As a result, the total energy of the complex is 28 kcal/mol worse than in the system with a remote drug.

To achieve this result, we imposed a limitation for argitoxin binding in the pore. To further check the possibility that an entire molecule of argitoxin can be accommodated in the cavity of the closed channel between the closed gate and the selectivity filter, we built a model with a sterically occluded selectivity filter. In this model the side chains of Gln586 formed a 16-membered cycle by side chain to side chain H-bonds. The dimensions of this cycle are too small to accommodate the tail of an argitoxin molecule.

We optimized this model and docked the argitoxin inside as described above. As expected, in the resulting low-energy structures the conformation of the argitoxin molecule was folded. Intraligand and intrareceptor energies were found to be significantly higher compared to the situation with a remote drug molecule (Table 1). It means that the placing of the toxin inside the cavity forces the ligand and the channel to adopt energetically unfavorable conformations. Essentially, the result is the same as in the original model with a constraint preventing the tail of the toxin molecule to penetrate the narrow part of the channel (see Table 1).

Thus, our modeling results suggest that effective binding of the argitoxin molecule in the closed AMPAR channel is possible only if the terminal part of the drug molecule penetrates the narrow channel part through the selectivity filter. Both attempts to dock the toxin molecule between the closed gate (bundle of M3 helices) and the selectivity filter (Gln 586 ring) resulted in much worse energetics, reflecting the fact that the central cavity of a closed channel is too small to accommodate the argitoxin molecule.

## DISCUSSION

In the present study we have demonstrated that argitoxin, which blocks the open AMPAR channel, is trapped in the closed channel after agonist removal. Modeling the argitoxin binding to the closed channel using recently published X-ray

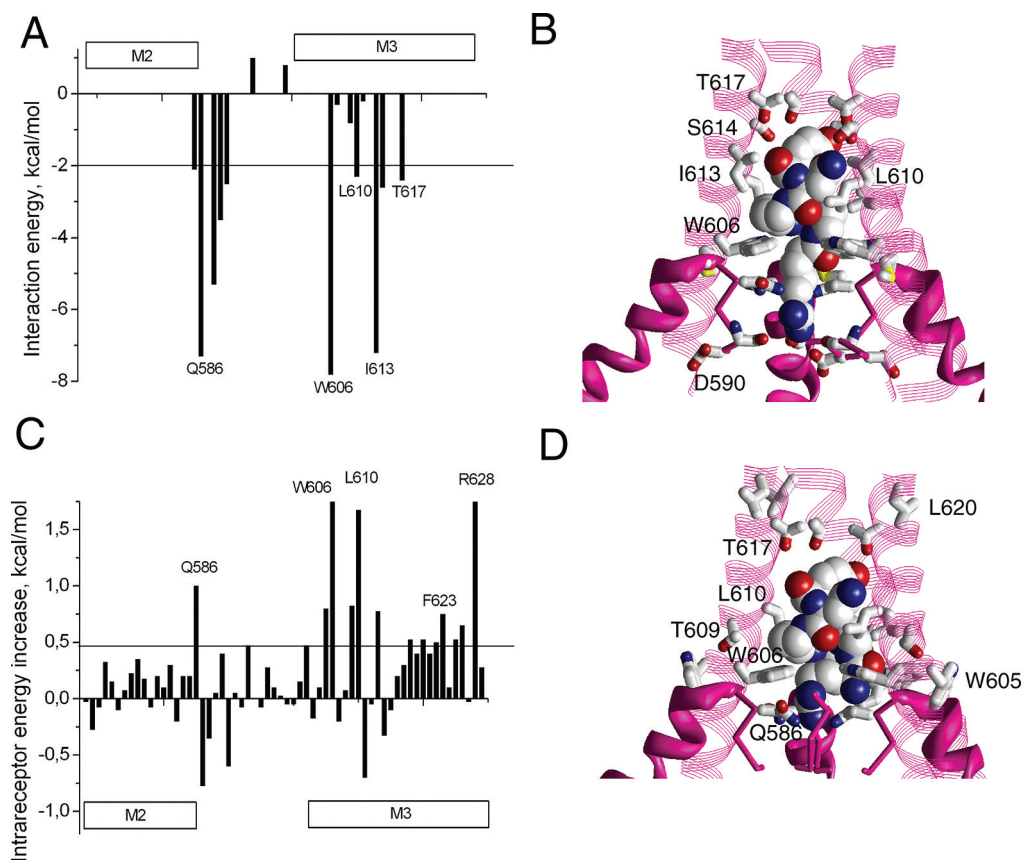


**Figure 4.** Partitioned energy of the argitoxin interaction with the closed AMPAR channel. (A) Contributions of the individual residues in the argitoxin–channel interactions as estimated from the unconstrained docking. (B) Spatial distributions of the residues, which contribute more than 2 kcal/mol. (C) Increase of the intrareceptor energy, partitioned by individual residues as estimated from the constrained docking. (D) Spatial distribution of the residues, with energies increased more than 0.5 kcal/mol.

data suggested that effective binding of the argitoxin in the closed AMPAR channel is possible only if the terminal guanidinium group of the drug penetrates into the narrow part of the channel below the selectivity filter. Taken together, the results suggest that the selectivity filter in the AMPAR channel is not sterically occluded when the channel is in the closed state.

In this work we assumed that the trapping blocking molecule does not prevent closure of the activation gate and that the cavity of the closed channel is large enough to accommodate the molecule. Such binding mode has been revealed for tetrabutylammonium in the closed KcsA channel.<sup>40</sup> Contrary, significant interaction with the channel gating machinery is believed to be responsible for the “foot-in-the-door” mechanism of blockade. In principle, it is possible that the binding energy of argitoxin in the closed AMPAR channel is weak, but the drug remains trapped simply because the closed gate occludes the exit pathway. If it were so, after the channel reopening the toxin would quickly leave the channel. However, recovery from block in trapping protocol was not faster than in the continuous presence of an agonist (see Figure 1D). This finding indicates that the closing of the AMPAR channel gate does not force the argitoxin to adopt a low-energy binding mode and supports our conclusion.

We did not consider the possibility that some argitoxin moieties could be located within the constriction of the M3 helices. The closed conformation of P-loop channels is stabilized in particular by tight interactions in the bundle of

M3 helices.<sup>41</sup> During the initial optimization of the AMPAR model we also found strong stabilizing contacts in the M3 segments. Our calculation demonstrated that location of argitoxin moieties within the constriction of M3 helices without displacing of the helices and destabilizing of the closed channel conformation is impossible. It should be noted that even single mutation in the M3 bundle destabilizes the closed channel significantly and results in spontaneous opening.<sup>3,37</sup> Certainly, by ruling out alternative models, we cannot ultimately prove our model of argitoxin binding. Such strong conclusions come only from direct experiments. However, in the absence of direct data the analysis of different possibilities using molecular modeling allows to find the most probable model, which can serve as working hypothesis for further studies.

For our analysis, we selected argitoxin because of the large size of its molecule. For smaller ligands, for example for philanthotoxin-343 or IEM-1925, modeling does not provide strong evidence. Small molecules can be forced to stay entirely in the cavity without steric hindrances. Conversely, the large size of the argitoxin molecule makes it a sensitive probe for the dimensions of the cavity of a closed AMPAR channel. Comparing the available X-ray structures of the closed AMPAR channel and the KcsA K<sup>+</sup> channel, we found significant difference in the positioning of the P-loops. The KcsA channel has been crystallized many times at different conditions. The P-loops in all available X-ray structures of the K<sup>+</sup> channels are very similar. The cause of the difference could be the limited

resolution of the AMPAR channel structure, or it could reflect a real structural difference between the channels. This important question requires further investigation. In our study we modeled the P-loops (M2 segments in glutamate receptors) as in the original work.<sup>5</sup> This choice does not affect our conclusions because in this case the central cavity is larger than in the KcsA structure. For a KcsA-like position of the P-loops our conclusion that the argiotoxin poorly fits the cavity of the closed channel would be even stronger.

Our present findings about the binding mode of argiotoxin in the closed AMPAR channel provide a new insight into our understanding of currently unresolved elements of the AMPAR channel structure and its mechanism of gating. Such knowledge is important for design of specific biochemical tools. It should be noted that our results do not rule out AMPAR gating at the level of the selectivity filter because the gating conformational changes do not necessarily involve steric pore occlusion. A disruption of the permeable conformation of the selectivity filter causing channel impermeability would be more likely.<sup>12,13</sup> We conclude that if any gating changes in the selectivity filter of AMPAR take place, they should be of similar character.

## AUTHOR INFORMATION

### Corresponding Author

\*Phone: 7- 812-552-3138. Fax: 7-812-55203012. E-mail: denistikhonov2002@yahoo.com.

## ACKNOWLEDGMENTS

This work was supported by the RFBR grant 10-04-00798-a, by the grants from Russian Academy of Sciences ("Molecular and Cell Biology" program) for D.B.T. and E.V.G., by the Russian Scientific Schools program (4419.2010.4) and by the Ministry of Education and Science of the Russian Federation (State contract No. 16.512.11.2197).

## ABBREVIATIONS

AMPAR,  $\alpha$ -amino-3-hydroxy-5-methyl-4-isoxazolepropionic acid receptor; MCM, Monte Carlo minimization.

## REFERENCES

- (1) Traynelis, S. F., Wollmuth, L. P., McBain, C. J., Menniti, F. S., Vance, K. M., Ogden, K. K., Hansen, K. B., Yuan, H., Myers, S. J., Dingledine, R., and Sibley, D. (2010) Glutamate receptor ion channels: structure, regulation, and function. *Pharmacol. Rev.* 62, 405–496.
- (2) Tikhonov, D. B. (2007) Ion channels of glutamate receptors: structural modeling. *Mol. Membr. Biol.* 24, 135–147.
- (3) Sobolevsky, A. I., Yelshansky, M. V., and Wollmuth, L. P. (2003) Different gating mechanisms in glutamate receptor and K<sup>+</sup> channels. *J. Neurosci.* 23, 7559–7568.
- (4) Wollmuth, L. P., and Sobolevsky, A. I. (2004) Structure and gating of the glutamate receptor ion channel. *Trends Neurosci.* 27, 321–328.
- (5) Sobolevsky, A. I., Rosconi, M. P., and Gouaux, E. (2009) X-ray structure, symmetry and mechanism of an AMPA-subtype glutamate receptor. *Nature* 462, 745–756.
- (6) Yuan, H., Erreger, K., Dravid, S. M., and Traynelis, S. F. (2005) Conserved structural and functional control of N-methyl-D-aspartate receptor gating by transmembrane domain M3. *J. Biol. Chem.* 280, 29708–29716.
- (7) Kohda, K., Wang, Y., and Yuzaki, M. (2000) Mutation of a glutamate receptor motif reveals its role in gating and delta2 receptor channel properties. *Nature Neurosci.* 3, 315–322.
- (8) Jones, K. S., VanDongen, H. M., and VanDongen, A. M. (2002) The NMDA receptor M3 segment is a conserved transduction element coupling ligand binding to channel opening. *J. Neurosci.* 22, 2044–2053.
- (9) Chang, H. R., and Kuo, C. C. (2008) The activation gate and gating mechanism of the NMDA receptor. *J. Neurosci.* 28, 1546–1556.
- (10) Zhou, Y., Morais-Cabral, J. H., Kaufman, A., and MacKinnon, R. (2001) Chemistry of ion coordination and hydration revealed by a K<sup>+</sup> channel-Fab complex at 2.0 Å resolution. *Nature* 414, 43–48.
- (11) Berneche, S., and Roux, B. (2005) A gate in the selectivity filter of potassium channels. *Structure* 13, 591–600.
- (12) Cuello, L. G., Jogini, V., Cortes, D. M., Pan, A. C., Gagnon, D. G., Dalmas, O., Cordero-Morales, J. F., Chakrapani, S., Roux, B., and Perozo, E. (2010) Structural basis for the coupling between activation and inactivation gates in K<sup>+</sup> channels. *Nature* 466, 272–275.
- (13) Cuello, L. G., Jogini, V., Cortes, D. M., and Perozo, E. (2010) Structural mechanism of C-type inactivation in K<sup>+</sup> channels. *Nature* 466, 203–208.
- (14) Beck, C., Wollmuth, L. P., Seeburg, P. H., Sakmann, B., and Kuner, T. (1999) NMDAR channel segments forming the extracellular vestibule inferred from the accessibility of substituted cysteines. *Neuron* 22, 559–570.
- (15) Sobolevsky, A. I., Beck, C., and Wollmuth, L. P. (2002) Molecular rearrangements of the extracellular vestibule in NMDAR channels during gating. *Neuron* 33, 75–85.
- (16) Antonov, S. M., Grishin, E. V., Magazanik, L. G., Shupliakov, O. V., Vesselkin, N. P., and Volkova, T. M. (1987) Argiopin blocks the glutamate responses and sensorimotor transmission in motoneurons of isolated frog spinal cord. *Neurosci. Lett.* 83, 179–184.
- (17) Budd, T., Clinton, P., Dell, A., Duce, I. R., Johnson, S. J., Quicke, D. L., Taylor, G. W., Usherwood, P. N., and Usoh, G. (1988) Isolation and characterisation of glutamate receptor antagonists from venoms of orb-weaver spiders. *Brain Res.* 448, 30–39.
- (18) Washburn, M. S., Numberger, M., Zhang, S., and Dingledine, R. (1997) Differential dependence on GluR2 expression of three characteristic features of AMPA receptors. *J. Neurosci.* 17, 9393–9406.
- (19) Raditsch, M., Geyer, M., Kalbitzer, H. R., Jahn, W., Ruppersberg, J. P., and Witzemann, V. (1996) Polyamine spider toxins and mammalian N-methyl-D-aspartate receptors. Structural basis for channel blocking and binding of argiotoxin636. *Eur. J. Biochem.* 240, 416–426.
- (20) Blagbrough, I. S., Brackley, P. T., Bruce, M., Bycroft, B. W., Mather, A. J., Millington, S., Sudan, H. L., and Usherwood, P. N. (1992) Arthropod toxins as leads for novel insecticides: an assessment of polyamine amides as glutamate antagonists. *Toxicol.* 30, 303–322.
- (21) Nelson, J. K., Frølund, S. U., Tikhonov, D. B., Kristensen, A. S., and Strømgaard, K. (2009) Synthesis and biological activity of argiotoxin 636 and analogues: selective antagonists for ionotropic glutamate receptors. *Angew. Chem., Int. Ed.* 48, 3087–3091.
- (22) Andersen, T. F., Tikhonov, D. B., Bølcho, U., Bolshakov, K., Nelson, J. K., Pluteanu, F., Mellor, I. R., Egebjerg, J., and Strømgaard, K. (2006) Uncompetitive antagonism of AMPA receptors: Mechanistic insights from studies of polyamine toxin derivatives. *J. Med. Chem.* 49, 5414–5423.
- (23) Donevan, S. D., and Rogawski, M. A. (1996) Multiple actions of arylalkylamine arthropod toxins on the N-methyl-D-aspartate receptor. *Neuroscience* 70, 361–375.
- (24) Priestley, T., Woodruff, G. N., and Kemp, J. A. (1989) Antagonism of responses to excitatory amino acids on rat cortical neurones by the spider toxin, argiotoxin636. *Br. J. Pharmacol.* 97, 1315–1323.
- (25) Brackley, P. T., Bell, D. R., Choi, S. K., Nakanishi, K., and Usherwood, P. N. (1993) Selective antagonism of native and cloned kainate and NMDA receptors by polyamine-containing toxins. *J. Pharmacol. Exp. Ther.* 266, 1573–1580.
- (26) Herlitz, S., Raditsch, M., Ruppersberg, J. P., Jahn, W., Monyer, H., Schoepfer, R., and Witzemann, V. (1993) Argiotoxin detects molecular differences in AMPA receptor channels. *Neuron* 10, 1131–1140.



- (27) Weiner, S. J., Kollman, P. A., Nguyen, D. T., and Case, D. A. (1986) An all atom force field for simulations of proteins and nucleic acids. *J. Comput. Chem.* 7, 230–252.
- (28) Lazaridis, T., and Karplus, M. (1999) Effective energy function for proteins in solution. *Proteins* 35, 133–152.
- (29) Dewar, M. J. S., Zoebisch, E. G., Healy, E. F., and Stewart, J. J. P. (1985) AM1: a new general purpose quantum mechanical model. *J. Am. Chem. Soc.* 107, 3902–3909.
- (30) Li, Z., and Scheraga, H. A. (1987) Monte Carlo-minimization approach to the multiple-minima problem in protein folding. *Proc. Natl. Acad. Sci. U. S. A.* 84, 6611–6615.
- (31) Mellor, I.R., and Usherwood, P. N. (2004) Targeting ionotropic receptors with polyamine-containing toxins. *Toxicon* 43, 493–508.
- (32) Bähring, R., and Mayer, M. L. (1998) An analysis of philanthotoxin block for recombinant rat GluR6(Q) glutamate receptor channels. *J. Physiol.* 509, 635–650.
- (33) Magazanik, L. G., Buldakova, S. L., Samoilova, M. V., Gmiro, V. E., Mellor, I. R., and Usherwood, P. N. (1997) Block of open channels of recombinant AMPA receptors and native AMPA/kainate receptors by adamantane derivatives. *J. Physiol.* 505, 655–663.
- (34) Doyle, D. A., Morais Cabral, J., Pfuetzner, R. A., Kuo, A., Gulbis, J. M., Cohen, S. L., Chait, B. T., and MacKinnon, R. (1998) The structure of the potassium channel: molecular basis of  $K^+$  conduction and selectivity. *Science* 280, 69–77.
- (35) Garden, D. P., and Zhorov, B. S. (2010) Docking flexible ligands in proteins with a solvent exposure- and distance-dependent dielectric function. *J. Comput.-Aided Mol. Des.* 24, 91–105.
- (36) Sobolevsky, A.I., Yelshansky, M. V., and Wollmuth, L. P. (2005) State-dependent changes in the electrostatic potential in the pore of a GluR channel. *Biophys. J.* 88, 235–242.
- (37) Kashiwagi, K., Masuko, T., Nguyen, C. D., Kuno, T., Tanaka, I., Igarashi, K., and Williams, K. (2002) Channel blockers acting at N-methyl-D-aspartate receptors: differential effects of mutations in the vestibule and ion channel pore. *Mol. Pharmacol.* 61, 533–545.
- (38) Kashiwagi, K., Williams, K., and Igarashi, K. (2007) Anthraquinone polyamines: novel channel blockers of N-methyl-D-aspartate receptors. *Amino Acids* 33, 299–304.
- (39) Tikhonov, D.B., Mellor, J. R., Usherwood, P. N., and Magazanik, L. G. (2002) Modeling of the pore domain of the GLUR1 channel: homology with  $K^+$  channel and binding of channel blockers. *Biophys. J.* 82, 1884–1893.
- (40) Zhou, M., Morais-Cabral, J. H., Mann, S., and MacKinnon, R. (2001) Potassium channel receptor site for the inactivation gate and quaternary amine inhibitors. *Nature* 411, 657–661.
- (41) Tikhonov, D. B., and Zhorov, B. S. (2004) In silico activation of KcsA  $K^+$  channel by lateral forces applied to the C-termini of inner helices. *Biophys. J.* 87, 1526–1536.